# Gravitational Instabilities in Gaseous Protoplanetary Disks and Implications for Giant Planet Formation

**Richard H. Durisen**
Indiana University

**Alan P. Boss**
Carnegie Institution of Washington

**Lucio Mayer**
Eidgenössische Technische Hochschule Zürich

**Andrew F. Nelson**
Los Alamos National Laboratory

**Thomas Quinn**
University of Washington

**W. K. M. Rice**
University of Edinburgh



Protoplanetary gas disks are likely to experience gravitational instabilites (GI's) during some phase of their evolution. Density perturbations in an unstable disk grow on a dynamic time scale into spiral arms that produce efficient outward transfer of angular momentum and inward transfer of mass through gravitational torques. In a cool disk with rapid enough cooling, the spiral arms in an unstable disk form self-gravitating clumps. Whether gas giant protoplanets can form by such a disk instability process is the primary question addressed by this review. We discuss the wide range of calculations undertaken by ourselves and others using various numerical techniques, and we report preliminary results from a large multi-code collaboration. Additional topics include – triggering mechanisms for GI's, disk heating and cooling, orbital survival of dense clumps, interactions of solids with GI-driven waves and shocks, and hybrid scenarios where GI's facilitate core accretion. The review ends with a discussion of how well disk instability and core accretion fare in meeting observational constraints.

## 1. INTRODUCTION

Gravitational instabilities (GI's) can occur in any region of a gas disk that becomes sufficiently cool or develops a high enough surface density. In the nonlinear regime, GI's can produce local and global spiral waves, self-gravitating turbulence, mass and angular momentum transport, and disk fragmentation into dense clumps and substructure. The particular emphasis of this review article is the possibility (*Kuiper*, 1951; *Cameron*, 1978), recently revived by *Boss* (1997, 1998a), that the dense clumps in a disk fragmented by GI's may become self-gravitating precursors to gas giant planets. This particular idea for gas giant planet formation has come to be known as the *disk instability* theory. We provide here a thorough review of the physics of GI's as currently understood through a wide variety of techniques and offer tutorials on key issues of physics and methodology. The authors assembled for this paper were deliberately chosen to represent the full range of views on the subject. Although we disagree about some aspects of GI's and about some interpretations of available results, we have labored hard to present a fair and balanced picture. Other recent reviews of this subject include *Boss* (2002c), *Durisen et al.* (2003), and *Durisen* (2006).

## 2. PHYSICS OF GI's

### 2.1 Linear Regime

The parameter that determines whether GI's occur in thin gas disks is

$$Q = c_s \kappa / \pi G \Sigma, \tag{1}$$

where $c_s$ is the sound speed, $\kappa$ is the epicyclic frequency at which a fluid element oscillates when perturbed from circular motion, $G$ is the gravitational constant, and $\Sigma$ is the surface density. In a nearly Keplerian disk, $\kappa \approx$ the rotational

angular speed $\Omega$. For axisymmetric (ring-like) disturbances, disks are stable when $Q > 1$ (*Toomre*, 1964). At high $Q$-values, pressure, represented by $c_s$ in (1), stabilizes short wavelengths, and rotation, represented by $\kappa$, stabilizes long wavelengths. The most unstable wavelength when $Q < 1$ is given by $\lambda_m \approx 2\pi^2 G\Sigma/\kappa^2$.

Modern numerical simulations, beginning with *Papaloizou and Savonije* (1991), show that nonaxisymmetric disturbances, which grow as multi-armed spirals, become unstable for $Q \lesssim 1.5$. Because the instability is both linear and dynamic, small perturbations grow exponentially on the time scale of a rotation period $P_{rot} = 2\pi/\Omega$. The multi-arm spiral waves that grow have a predominantly trailing pattern, and several modes can appear simultaneously (*Boss*, 1998a; *Laughlin et al.*, 1998; *Nelson et al.*, 1998; *Pickett et al.*, 1998). Although the star does become displaced from the system center of mass (*Rice et al.*, 2003a) and one-armed structures can occur (see Fig. 1 of *Cai et al.*, 2006), one-armed modes do not play the dominant role predicted by *Adams et al.* (1989) and *Shu et al.* (1990).

### 2.2 Nonlinear Regime

Numerical simulations (see also Sections 3 and 4) show that, as GI's emerge from the linear regime, they may either saturate at nonlinear amplitude or fragment the disk. Two major effects control or limit the outcome – disk thermodynamics and nonlinear mode coupling. At this point, the disks also develop large surface distortions.

Disk Thermodynamics. As the spiral waves grow, they can steepen into shocks that produce strong localized heating (*Pickett et al.*, 1998, 2000a; *Nelson et al.*, 2000). Gas is also heated by compression and through net mass transport due to gravitational torques. The ultimate source of GI heating is work done by gravity. What happens next depends on whether a balance can be reached between heating and the loss of disk thermal energy by radiative or convective cooling. The notion of a balance of heating and cooling in the nonlinear regime was described as early as 1965 by *Goldreich and Lynden-Bell* and has been used as a basis for proposing $\alpha$-treatments for GI-active disks (*Paczyński*, 1978; *Lin and Pringle*, 1987). For slow to moderate cooling rates, numerical experiments, such as in Fig. 1, verify that thermal self-regulation of GI's can be achieved (*Tomley et al.*, 1991; *Pickett et al.*, 1998, 2000a, 2003; *Nelson et al.*, 2000; *Gammie*, 2001; *Boss*, 2003; *Rice et al.*, 2003b; *Lodato and Rice*, 2004, 2005; *Mejía et al.* 2005; *Cai et al.*, 2006). $Q$ then hovers near the instability limit, and the nonlinear amplitude is controlled by the cooling rate.

Nonlinear Mode Coupling. Using second and third-order governing equations for spiral modes and comparing their results with a full nonlinear hydrodynamics treatment, *Laughlin et al.* (1997, 1998) studied nonlinear mode coupling in the most detail. Even if only a single mode initially emerges from the linear regime, power is quickly distributed over modes with a wide variety of wavelengths and number of arms, resulting in a self-gravitating turbulence

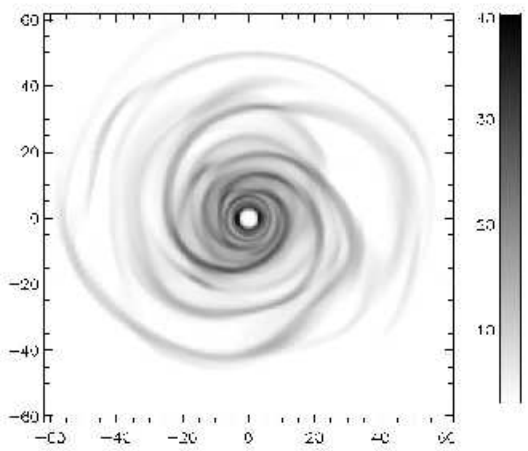


Fig. 1.— Greyscale of effective temperature $T_{eff}$ in degrees Kelvin for a face-on GI-active disk in an asymptotic state of thermal self-regulation. This figure is for the *Mejía et al.* (2005) evolution of a 0.07 $M_\odot$ disk around a 0.5 $M_\odot$ star with $t_{cool} = 1$ outer rotation period at 4,500 yr. The frame is 120 AU on a side.

that permeates the disk. In this *gravitoturbulence*, gravitational torques and even Reynold's stresses may be important over a wide range of scales (*Nelson et al.*, 1998; *Gammie*, 2001; *Lodato and Rice*, 2004; *Mejía et al.*, 2005).

Surface Distortions. As emphasized by *Pickett et al.* (1998, 2000, 2003), the vertical structure of the disk plays a crucial role, both for cooling and for essential aspects of the dynamics. There appears to be a relationship between GI spiral modes and the surface or f-modes of stratified disks (*Pickett et al.*, 1996; *Lubow and Ogilvie*, 1998). As a result, except for isothermal disks, GI's tend to have large amplitudes at the surface of the disk. Shock heating in the GI spirals can also disrupt vertical hydrostatic equilibrium, leading to rapid vertical expansions that resemble hydraulic jumps (*Boley et al.*, 2005; *Boley and Durisen*, 2006). The resulting spiral corrugations can produce observable effects (e.g., masers, *Durisen et al.*, 2001).

### 2.3 Heating and Cooling

Protoplanetary disks are expected to be moderately thin, with $H/r \sim 0.05 - 0.1$, where $H$ is the vertical scale height and $r$ is the distance from the star. For hydrostatic equilibrium in the vertical direction, $H \approx c_s/\Omega$. The ratio of disk internal energy to disk binding energy $\sim {c_s}^2/(r\Omega)^2 \sim (H/r)^2$ is then $\lesssim 1\%$. As growing modes become nonlinear, they tap the enormous store of gravitational energy in the disk. Simulation of the disk energy budget must be done accurately and include all relevant effects, because it is the disk temperature, through $c_s$ in equation 1, that determines whether the disk becomes or remains unstable, once the central mass, which governs most of $\kappa$, and

the disk mass distribution $\Sigma$ have been specified.

*2.3.1 Cooling*

There have been three approaches to cooling – make simple assumptions about the equation of state (EOS), include idealized cooling characterized by a cooling time, or treat radiative cooling using realistic opacities.

EOS. This approach has been used to study mode coupling (e.g., *Laughlin et al.*. 1998) and to examine disk fragmentation in the limits of isentropic and isothermal behavior (e.g., *Boss*, 1998a, 2000; *Nelson et al.*, 1998; *Pickett et al.*, 1998, 2003; *Mayer et al.*, 2004). Isothermal evolution of a disk, where the disk temperature distribution is held fixed in space or when following fluid elements, effectively assumes rapid loss of energy produced by shocks and $PdV$ work. Isentropic evolution, where specific entropy is held fixed instead of temperature, is a more moderate assumption but is still lossy because it ignores entropy generation in shocks (*Pickett et al.*, 1998, 2000a). Due to the energy loss, we do not refer to such calculations as adiabatic. Here, we restrict *adiabatic evolution* to mean cases where the fluid is treated as an ideal gas with shock heating included via an artificial viscosity term in the internal energy equation but no radiative cooling. Such calculations are adiabatic in the sense that there is no energy loss by the system. Examples include a simulation in *Pickett et al.* (1998) and simulations in *Mayer et al.* (2002, 2004). *Mayer et al.* use adiabatic evolution throughout some simulations, but, in others that are started with a locally isothermal EOS, they switch to adiabatic evolution as the disk approaches fragmentation.

Simple Cooling Laws. Better experimental control over energy loss is obtained by adopting simple cooling rates per unit volume $\Lambda = \epsilon/t_{cool}$, where $\epsilon$ is the internal energy per unit volume. The $t_{cool}$ is specified either as a fixed fraction of the local disk rotation period $P_{rot}$, usually by setting $t_{cool}\Omega =$ constant (*Gammie*, 2001; *Rice et al.*, 2003b; *Mayer et al.*, 2004b, 2005) or $t_{cool} =$ constant everywhere (*Pickett et al.*, 2003; *Mejía et al.*, 2005). In the *Mayer et al.* work, the cooling is turned off in dense regions to simulate high optical depth. Regardless of $t_{cool}$ prescription, the amplitude of the GI's in the *asymptotic state* (see Fig. 1), achieved when heating and cooling are balanced, increases as $t_{cool}$ decreases. In addition to elucidating the general physics of GI's, such studies address whether GI's are intrinsically a local or global phenomenon (*Laughlin and Różyczka* 1996; *Balbus and Papaloizou*, 1999) and whether they can be properly modeled by a simple $\alpha$ prescription. When $t_{cool}$ is globally constant, the transport induced by GI's is global with high mass inflow rates (*Mejía et al.*, 2005; *Michael et al.*, in preparation); when $t_{cool}\Omega$ is constant, transport is local, except for thick or very massive disks, and the inflow rates are well characterized by a constant $\alpha$ (*Gammie*, 2001; *Lodato and Rice*, 2004, 2005).

Radiative Cooling. The published literature on this so far comes from only three research groups (*Nelson et al.*, 2000; *Boss*, 2001, 2002b, 2004a; *Mejía*, 2004; *Cai et al.*, 2006), but work by others is in progress. Because Solar System-sized disks encompass significant volumes with small and large optical depth, this becomes a difficult 3D radiative hydrodynamics problem. Techniques will be discussed in Section 3.2. For a disk spanning the conventional planet-forming region, the opacity is due primarily to dust. Complications which have to be considered include the dust size distribution, its composition, grain growth and settling, and the occurrence of fast cooling due to convection.

In general, the radiative cooling time is dependent on temperature $T$ and metallicity $Z$. Let $\kappa_r \sim ZT^{\beta_r}$ and $\kappa_p \sim ZT^{\beta_p}$ be the Rosseland and Planck mean opacities, respectively, and let $\tau \sim \kappa_r H$ be the vertical optical depth to the midplane. For large $\tau$,

$$t_{cool} \sim T/{T_{eff}}^4 \sim T^{-3}\tau \sim T^{-2.5+\beta_r}Z; \qquad (2)$$

for small $\tau$,

$$t_{cool} \sim T/\kappa_p T^4 \sim T^{-3-\beta_p}/Z. \qquad (3)$$

For most temperatures regimes, we expect $-3 < \beta < 2.5$, so that $t_{cool}$ increases as $T$ decreases. As $Z$ increases, $t_{cool}$ increases in optically thick regions, but decreases in optically thin ones.

*2.3.2 Heating*

In addition to the internal heating caused by GI's through shocks, compression, and mass transport, there can be heating due to turbulent dissipation (*Nelson et al.*, 2000) and other sources of shocks. In addition, a disk may be exposed to one or more external radiation fields due to a nearby OB star (e.g., *Johnstone et al.*, 1998), an infalling envelope (e.g., *D'Alessio et al.*, 1997), or the central star (e.g., *Chiang and Goldreich*, 1997). These forms of heat input can be comparable to or larger than internal sources of heating and can influence $Q$ and the surface boundary conditions. Only crude treatments have been done so far for envelope irradiation (*Boss* 2001, 2002b; *Cai et al.*, 2006) and for stellar irradiation (*Mejía*, 2004).

### 2.4 Fragmentation

As shown first by *Gammie* (2001) for local thin-disk calculations and later confirmed by *Rice et al.* (2003b) and *Mejía et al.* (2005) in full 3D hydro simulations, disks with a fixed $t_{cool}$ fragment for sufficiently fast cooling, specifically when $t_{cool}\Omega \lesssim 3$, or, equivalently, $t_{cool} \lesssim P_{rot}/2$. Finite thickness has a slight stabilizing influence (*Rice et al.*, 2003b; *Mayer et al.*, 2004a). When dealing with realistic radiative cooling, one cannot apply this simple fragmentation criterion to arbitrary initial disk models. One has to apply it to the asymptotic phase after nonlinear behavior is well-developed (*Johnson and Gammie*, 2003). Cooling times can be much longer in the asymptotic state than they are initially (*Cai et al.*, 2006, *Mejía et al.*, in preparation). For disks evolved under isothermal conditions, where a simple cooling time cannot be defined, local thin-disk calculations show fragmentation when $Q \lesssim 1.4$ (*Johnson and Gammie*, 2003). This is roughly consistent with results from global simulations (e.g., *Boss*, 2000; *Nelson et al.*, 1998; *Pickett et*

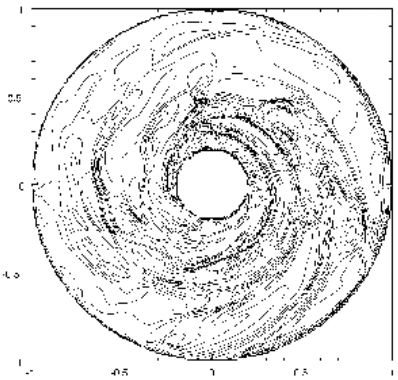

Fig. 2.— Midplane density contours for the isothermal evolution of a 0.09 $M_\odot$ disk around a 1 $M_\odot$ star. A multi-Jupiter mass clump forms near 12 o'clock by 374 years. The frame in the figure is 40 AU on a side. The figure is adapted from *Boss* (2000).

*al.*, 2000a, 2003; *Mayer et al.*, 2002, 2004a). Fig. 2 shows a classic example of a fragmenting disk.

Although there is agreement on conditions for fragmentation, two important questions remain. Do real disks ever cool fast enough for fragmentation to occur, and do the fragments last long enough to contract into permanent protoplanets before being disrupted by tidal stresses, shear stresses, physical collisions, and shocks?

## 3. NUMERICAL METHODS

A full understanding of disk evolution and the planet formation process cannot easily be obtained using a purely analytic approach. Although numerical methods are powerful, they have flaws and limitations that must be taken into account when interpreting results. Here we describe some commonly used numerical techniques and their limitations.

### 3.1 Hydrodynamics

Numerical models have been implemented using one or the other of two broad classes of techniques to solve the hydrodynamic equations. Each class discretizes the system in fundamentally different ways. On one hand, there are particle-based simulations using Smoothed Particle Hydrodynamics (SPH) (*Benz*, 1990; *Monaghan*, 1992), and, on the other, grid-based techniques (e.g., *Tohline*, 1980; *Fryxell et al.*, 1991; *Stone and Norman*, 1992; *Boss and Myhill*, 1992; *Pickett*, 1995).

SPH uses a collection of particles distributed in space to represent the fluid. Each particle is free to move in response to forces acting on it, so that the particle distribution changes with the system as it evolves. The particles are collisionless, meaning that they do not represent actual physical entities, but rather points at which the underlying distributions of mass, momentum, and energy are sampled. In order to calculate hydrodynamic quantities such as mass density or pressure forces, contributions from other particles within a specified distance, the *smoothing length*, are weighted according to a *smoothing kernel* and summed in pairwise fashion. Mutual gravitational forces are calculated by organizing particles into a tree, where close particles are treated more accurately than aggregates on distant branches.

Grid-based methods use a grid of points, usually fixed in space, on which fluid quantities are defined. In the class of *finite difference* schemes, fluxes of mass, momentum, and energy between adjacent cells are calculated by taking finite differences of the fluid quantities in space. Although not commonly used in simulations of GI's, the Piecewise Parabolic Method (PPM) of *Collela and Woodward* (1984) represents an example of the class of *finite volume* schemes. For our purposes, an important distinguishing factor is that while finite difference and SPH methods may require artificial viscosity terms to be added to the equations to ensure numerical stability and produce correct dissipation in shocks, PPM does not.

### 3.2 Radiative Physics

In Section 2.3, we describe a number of processes by which disks may heat and cool. In this section, we discuss various code implementations and their limitations.

Fixed EOS evolution is computationally efficient because it removes the need to solve an equation for the energy balance. On the other hand, the gas instantly radiates away all heating due to shocks and, for the isothermal case, due to compressional heating as well. As a consequence, the gas may compress to much higher densities than are realistic, biasing a simulation towards GI growth and fragmentation even when a physically appropriate temperature or entropy scale is used. Although fixed $t_{cool}$'s represent a clear advance over fixed EOS's, equations 2 and 3 show that increasing the temperature, which makes the disk more stable, also decreases $t_{cool}$. So it is incorrect to view short global cooling times as necessarily equivalent to more rapid GI growth and fragmentation. In order for fragmentation to occur, one needs *both* a short $t_{cool}$ *and* a disk that is cool enough to be unstable (e.g., *Rafikov*, 2005).

The most physically inclusive simulations to date employ radiative transport schemes that allow $t_{cool}$ to be determined by disk opacity. Current implementations (Section 2.3) employ variants of a radiative diffusion approximation in regions of medium to high optical depth $\tau$, integrated from infinity toward the disk midplane. On the other hand, radiative losses actually occur from regions where $\tau \lesssim 1$, and so the treatment of the interface between optically thick and thin regions strongly influences cooling. Three groups have implemented different approaches.

*Nelson et al.* (2000) assume that the vertical structure of the disk can be defined at each point as an atmosphere in thermal equilibrium. In this limit, the interface can be defined by the location of the disk *photosphere*, where $\tau = 2/3$ (see, e.g., *Mihalas*, 1977). Cooling at each point is then defined as that due to a blackbody with the temper-

ature of the photosphere. *Boss* (2001, 2002b, 2004a, 2005) performs a 3D flux-limited radiative diffusion treatment for the optically thick disk interior (*Bodenheimer et al.*, 1990), coupled to an outer boundary condition where the temperature is set to a constant for $\tau < 10$, $\tau$ being measured along the radial direction. *Mejía* (2004) and *Cai et al.* (2006) use the same radiative diffusion treatment as *Boss* in their disk interior, but they define the interface using $\tau = 2/3$, measured vertically, above which an optically thin atmosphere model is self-consistently grafted onto the outward flux from the interior. As discussed in Section 4.2, results for the three groups differ markedly, indicating that better understanding of radiative cooling at the disk surface will be required to determine the fate of GI's.

### 3.3 Numerical Issues

The most important limitations facing numerical simulations are finite computational resources. Simulations have a limited duration with a finite number of particles or cells, and they must have boundary conditions to describe behavior outside the region being computed. A simulation must distribute grid cells or particles over the interesting parts of the system to resolve the relevant physics and avoid errors associated with incorrect treatment of the boundaries. Here we describe a number of requirements for valid simulations and pitfalls to be avoided.

For growth of GI's, simulations must be able to resolve the wavelengths of the instabilities underlying the fragmentation. *Bate and Burkert* (1997) and *Truelove et al.* (1997) each define criteria based on the collapse of a Jeans unstable cloud that links a minimum number of grid zones or particles to either the physical wavelength or mass associated with Jeans collapse. *Nelson* (2006) notes that a Jeans analysis may be less relevant for disk systems because they are flattened and rotating rather than homogeneous and instead proposes a criterion based on the Toomre wavelength in disks. Generally, grid-based simulations must resolve the appropriate local instability wavelength with a minimum of 4 to 5 grid zones in each direction, while SPH simulations must resolve the local Jeans or Toomre mass with a minimum of a few hundred particles.

Resolution of instability wavelengths will be insufficient to ensure validity if either the hydrodynamics or gravitational forces are in error. For example, errors in the hydrodynamics may develop in SPH and finite difference methods because a viscous heating term must be added artificially to model shock dissipation and, in some cases, to ensure numerical stability. In practice, the magnitude of dissipation depends in part on cell dimensions rather than just on physical properties. Discontinuities may be smeared over as many as $\sim 10$ or more cells, depending on the method. Further, *Mayer et al.* (2004a) have argued that because it takes the form of an additional pressure, artificial viscosity may by itself reduce or eliminate fragmentation. On the other hand, artificial viscosity can promote the longevity of clumps (see Fig. 3 of *Durisen*, 2006).

Gravitational force errors develop in grid simulations from at least two sources. First, when *Pickett et al.* (2003) place a small blob within their grid, errors occur in the self-gravitation force of the blob that depend on whether the cells containing it have the same spacing in each coordinate dimension. Ideally, grid zones would have comparable spacing in all directions, but disks are both thin and radially extended. Use of spherical and cylindrical grids tends to introduce disparity in grid spacing. Second, *Boss* (2000) shows that maximum densities inside clumps are enhanced by orders of magnitude as additional terms in his Poisson solver, based on a $Y_{lm}$ decomposition, are included. SPH simulations encounter a different source of error because gravitational forces must be softened in order to preserve the collisionless nature of the particles. *Bate and Burkert* (1997) and *Nelson* (2006) each show that large imbalances between the gravitational and pressure forces can develop if the length scales for each are not identical, possibly inducing fragmentation in simulations. On the other hand, spatially and temporally variable softening implies a violation of energy conservation. Quantifying errors from sources such as insufficiently resolved shock dissipation or gravitational forces cannot be reliably addressed except by experimentation. Results of otherwise identical simulations performed at several resolutions must be compared, and identical models must be realized with more than one numerical method (as in Section 4.4), so that deficiencies in one method can be checked against strengths in another.

The disks relevant for GI growth extend over several orders of magnitude in radial range, while GI's may develop large amplitudes only over some fraction of that range. Computationally affordable simulations therefore require both inner and outer radial boundaries, even though the disk may spread radially and spiral waves propagate up to or beyond those boundaries. In grid-based simulations, *Pickett et al.* (2000b) demonstrate that numerically induced fragmentation can occur with incorrect treatment of the boundary. Studies of disk evolution must ensure that treatment of the boundaries does not produce artificial effects.

In particle simulations, where there is no requirement that a grid be fixed at the beginning of the simulation, boundaries are no less a problem. The smoothing in SPH requires that the distribution of neighbors over which the smoothing occurs be relatively evenly distributed in a sphere around each particle for the hydrodynamic quantities to be well defined. At currently affordable resolutions ($\sim 10^5 - 10^6$ particles), the smoothing kernel extends over a large fraction of a disk scale height, so meeting this requirement is especially challenging. Impact on the outcomes of simulations has not yet been quantified.

## 4. KEY ISSUES

### 4.1 Triggers for GI's

When disks become unstable, they may either fragment or enter a self-regulated phase depending on the cooling

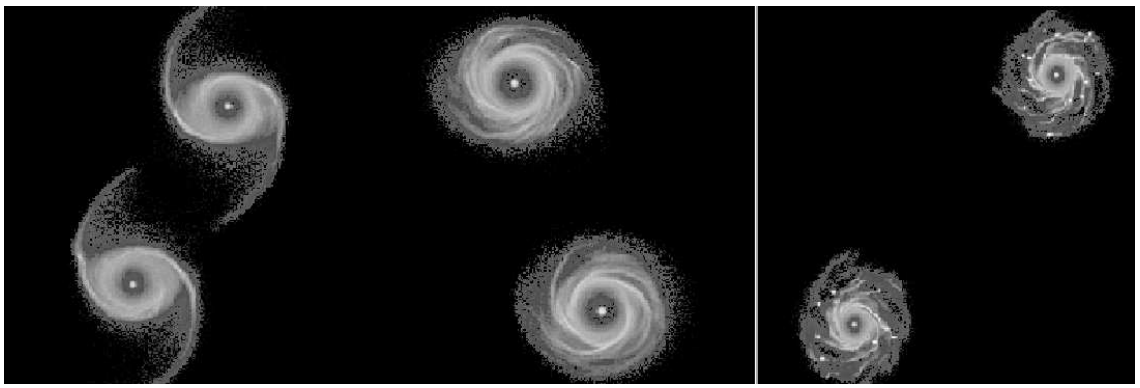

Fig. 3.— Face-on density maps for two simulations of interacting $M = 0.1M_{\odot}$ protoplanetary disks in binaries with $t_{cool} = 0.5P_{rot}$ viewed face-on. The binary in the left panel has a nearly circular binary orbit with an initial separation of 60 AU and is shown after first pericentric passage at 150 yrs (left) and then at 450 yrs (right). Large tidally induced spiral arms are visible at 150 yrs. The right panel shows a snapshot at 160 yrs from a simulation starting from an initial orbital separation that is twice as large. In this case, fragmentation into permanent clumps occurs after a few disk orbital times. Figures adapted from *Mayer et al.* (2005).

time. It is therefore important to know how and when GI's may arise in real disks and the physical state of the disk at that time. Various mechanisms for triggering GI's are conceivable, but only a few have yet been studied in any detail. Possibilities include – the formation of a massive disk from the collapse of a protostellar cloud (e.g., *Laughlin and Bodenheimer*, 1994; *Yorke and Bodenheimer*, 1999), clumpy infall onto a disk (*Boss*, 1997, 1998a), cooling of a disk from a stable to an unstable state, slow accretion of mass, accumulation of mass in a magnetically dead zone, perturbations by a binary companion, and close encounters with other star/disk systems (*Boffin et al.*, 1998; *Lin et al.*, 1998). A few of these will be discussed further, with an emphasis on some new results on effects of binarity.

Several authors start their disks with stable or marginally stable $Q$-values and evolve them to instability either by slow idealized cooling (e.g., *Gammie*, 2001; *Pickett et al.*, 2003; *Mejía et al.*, 2005) or by more realistic radiative cooling (e.g., *Johnson and Gammie*, 2003; *Boss*, 2005, 2006; *Cai et al.*, 2006). To the extent tested, fragmentation in idealized cooling cases are consistent with the Gammie criterion (Section 2.4). With radiative cooling, as first pointed out by *Johnson and Gammie* (2003), it is difficult to judge whether a disk will fragment when it reaches instability based on its initial $t_{cool}$. When *Mayer et al.* (2004a) grow the mass of a disk while keeping its temperature constant, dense clumps form in a manner similar to clump formation starting from an unstable disk. A similar treatment of accretion needs to be done using realistic radiative cooling. Simulations like these suggest that, in the absence of a strong additional source of heating, GI's are unavoidable in protoplanetary disks with sufficient mass ($\sim 0.1M_{\odot}$ for a $\sim 1M_{\odot}$ star).

A disk evolving primarily due to magnetorotational instabilites (MRI's) may produce rings of cool gas in the disk midplane where the ionization fraction drops sufficiently to quell MRI's (*Gammie*, 1996; *Fleming and Stone*, 2003). Dense rings associated with these magnetically *dead zones* should become gravitationally unstable and may well trigger a localized onset of GI's. This process might lead to disk outbursts related to FU Orionis events (*Armitage et al.*, 2001) and induce chondrule-forming episodes (*Boley et al.*, 2005).

A phase of GI's robust enough to lead to gas giant protoplanet formation might be achieved through external triggers, like a binary star companion or a close encounter with another protostar and its disk. A few studies have explored the effects of binary companions on GI's. *Nelson* (2000) follows the evolution of disks in an equal-mass binary system with a semimajor axis of 50 AU and an eccentricity of 0.3 and finds that the disks are heated by internal shocks and viscous processes to such an extent as to become too hot for gas giant planet formation either by disk GI's or by core accretion, because volatile ices and organics are vaporized. In a comparison of the radiated emission calculated from his simulation to those from the L1551 IRS5 system, *Nelson* (2000) finds that the simulation is well below the observed system and therefore that the temperatures in the simulation are underestimates. He therefore concludes that "planet formation is unlikely in equal-mass binary systems with $a \sim$ 50 AU." Currently, over two dozen binary or triple star systems have known extrasolar planets, with binary separations ranging from $\sim 10$ AU to $\sim 10^3$ AU, so some means must be found for giant planet formation in binary star systems with relatively small semimajor axes.

Using idealized cooling, *Mayer et al.* (2005) find that the effect of binary companions depends on the mass of the disks involved and on the disk cooling rate. For a pair of massive disks ($M \sim 0.1M_{\odot}$), formation of permanent clumps can be suppressed as a result of intense heating from spiral shocks excited by the tidal perturbation (Fig. 3 left panel). Clumps do not form in such disks for binary orbits having a semimajor axis of $\sim 60$ AU even when $t_{cool} < P_{rot}$. The temperatures reached in these disks are $> 200$ K and would vaporize water ice, hampering core ac-

cretion, as argued by *Nelson* (2000). On the other hand, pairs of less massive disks ($M \sim 0.05 M_{\odot}$) that would not fragment in isolation since they start with $Q \sim 2$, can produce permanent clumps provided that $t_{cool} \lesssim P_{rot}$. This is because the tidal perturbation is weaker in this case (each perturber is less massive) and the resulting shock heating is thus diminished. Finally, the behavior of such binary systems approaches that seen in simulations of isolated disks once the semimajor axis grows beyond $100$ AU (Fig. 3 right panel).

Calculations by *Boss* (2006) of the evolution of initially marginally gravitationally stable disks show that the presence of a binary star companion could help to trigger the formation of dense clumps. The most likely explanation for the difference in outcomes between the models of *Nelson* (2000) and *Boss* (2006) is the relatively short cooling times in the latter models ($\sim 1$ to 2 $P_{rot}$, see *Boss* 2004a) compared to the effective cooling time in *Nelson* (2000) of $\sim 15 P_{rot}$ at 5 AU, dropping to $\sim P_{rot}$ at 15 AU. Similarly, some differences in outcomes between the results of *Boss* (2006) and *Mayer et al.* (2005) can be expected based on different choices of the binary semimajor axes and eccentricities and differences in the thermodynamics. For example, *Mayer et al.* (2005) turn off cooling in regions with densities higher than $10^{-10}$ g cm$^{-3}$ to account for high optical depths.

Overall, the three different calculations agree that excitation or suppression of fragmentation by a binary companion depends sensitively on the balance between compressional/shock heating and cooling. This balance appears to depend on the mass of the disks involved. Interestingly, lighter disks are more likely to fragment in binary systems according to both *Mayer et al.* (2005) and *Boss* (2006).

### 4.2 Disk Thermodynamics

As discussed in Sections 2.2 and 4.1, heating and cooling are perhaps the most important processes affecting the growth and fate of GI's. Thermal regulation in the nonlinear regime leads naturally to systems near their stability limit where temporary imbalances in one heating or cooling term lead to a proportionate increase in a balancing term. For fragmentation to occur, a disk must cool quickly enough, or fail to be heated for long enough, to upset this self-regulation. A complete model of the energy balance that includes all relevant processes in a time-dependent manner is beyond the capabilities of the current generation of models. It requires knowledge of all the following – external radiation sources and their influence on the disk at each location, the energy lose rate of the disk due to radiative cooling, dynamical processes that generate thermal energy through viscosity or shocks, and a detailed equation of state to determine how much heating any of those dynamical processes generate. Recent progress towards understanding disk evolution has focused on the more limited goals of quantifying the sensitivity of results to various processes in isolation.

In a thin, steady state $\alpha$-disk, the heating and cooling times are the same and take a value (*Pringle*, 1981; *Gammie*, 2001):

$$t_{cool} = \frac{4}{9} \left[\gamma(\gamma - 1)\alpha\Omega\right]^{-1} . \quad (4)$$

For $\alpha \sim 10^{-2}$ and $\gamma = 1.4$, equation 4 gives $\sim 12 P_{rot}$. This is a crude upper limit on the actual time scale required to change the disk thermodynamic state. External radiative heating from the star and any remaining circumstellar material can contribute a large fraction of the total heating (*D'Alessio et al.*, 1998; *Nelson et al.*, 2000), as will any internal heating due to globally generated dynamical instabilities that produce shocks. Each of these processes actually makes the disk more stable by heating it, but, as a consequence, dynamical evolution slows until the disk gains enough mass to become unstable again. The marginally stable state will then be precariously held because the higher temperatures mean that all of the heating and cooling time scales, i.e., the times required to remove or replace all the disk thermal energy, are short (equations 2 and 3). When the times are short, any disruption of the contribution from a single source may be able to change the thermodynamic state drastically within only a few orbits, perhaps beyond the point where balance can be restored.

A number of models (Section 2.3) have used fixed EOS evolution instead of a full solution of an energy equation to explore disk evolution. A fixed EOS is equivalant to specifying the outcomes of all heating and cooling events that may occur during the evolution, short-circuiting thermal feedback. If, for example, the temperature or entropy is set much too high or too low, a simulation may predict either that no GI's develop in a system, or that they inevitably develop and produce fragmentation, respectively. Despite this limitation, fixed EOS's have been useful to delineate approximate boundaries for regions of marginal stability. Since the thermal state is fixed, disk stability (as quantified by equation 1) is essentially determined by the disk's mass and spatial dimensions, though its surface density. Marginal stability occurs generally at $Q \approx 1.2$ to 1.5 for locally isentropic evolutions, with a tendency for higher $Q$'s being required to ensure stability with *softer* EOS's (i.e., with lower $\gamma$ values) (*Boss* 1998a; *Nelson et al.*, 1998; *Pickett et al.*, 1998, 2000a; *Mayer et al.*, 2004a). At temperatures appropriate for observed systems (e.g., *Beckwith et al.*, 1990), these $Q$ values correspond to disks more massive than $\sim 0.1 M_*$ or surface densities $\Sigma \gtrsim 10^3$ gm/cm$^2$.

As with their fixed EOS cousins, models with fixed $t_{cool}$ can quantify boundaries at which fragmentation may set in. They represent a clear advance over fixed EOS evolution by allowing thermal energy generated by shocks or compression to be retained temporarily, and thereby enabling the disk's natural thermal regulation mechanisms to determine the evolution. Models that employ fixed cooling times can address the question of how violently the disk's thermal regulation mechanisms must be disrupted before they can no longer return the system to balance. An example of the value of fixed $t_{cool}$ calculations is the fragmentation

criterion $t_{cool} \lesssim 3\Omega^{-1}$ (see Section 2.4).

The angular momentum transport associated with disk self-gravity is a consequence of the gravitational torques induced by GI spirals (e.g., *Larson*, 1984). The viscous $\alpha$ parameter is actually a measure of that stress normalized by the local disk pressure. As shown in equation 4 and reversing the positions of $t_{cool}$ and $\alpha$, the stress in a self-gravitating disk depends on the cooling time and on the equation of state through the specific heat ratio. As long as the dimensionless scale height is $H \lesssim 0.1$, global simulations by *Lodato and Rice* (2004) with $t_{cool}\Omega =$ constant confirm Gammie's assumption that transport due to disk self-gravity can be modeled as a local phenomenon and that equation 4 is accurate. *Gammie* (2001) and *Rice et al.* (2005) show that there is a maximum stress that can be supplied by such a quasi-steady, self-gravitating disk. Fragmentation occurs if the stress required to keep the disk in a quasi-steady state exceeds this maximum value. The relationship between the stress and the specific heat ratio, $\gamma$, results in the cooling time required for fragmentation increasing as $\gamma$ decreases. For $\gamma = 7/5$, the cooling time below which fragmentation occurs may be more like $2P_{rot}$, not the $3/\Omega \approx P_{rot}/2$ obtained for $\gamma = 2$ (*Gammie*, 2001; *Mayer et al.*, 2004b; *Rice et al.*, 2005).

Important sources of stress and heating in the disk, that lie outside the framework of Gammie's local analysis, are global gravitational torques due to low-order GI spiral modes. There are two ways this can happen – a geometrically thick massive disk (*Lodato and Rice*, 2005) and a fixed global $t_{cool}$ = constant (*Mejía et al.*, 2005). Disks then initially produce large-amplitude spirals, resulting in a transient burst of global mass and angular momentum redistribution. For $t_{cool}$ = constant and moderate masses, the disks then settle down to a self-regulated asymptotic state but with gravitational stresses significantly higher than predicted by equation 4 (*Michael et al.*, in preparation). For the very massive $t_{cool}\Omega =$ constant disks, recurrent episodic redistributions occur. In all these cases, the heating in spiral shocks is spatially and temporally very inhomogeneous, as are fluctuations in all thermodynamic variables and the velocity field.

The most accurate method to determine the internal thermodynamics of the disk is to couple the equations of radiative transport to the hydrodynamics directly. All heating or cooling due to radiation will then be properly defined by the disk opacity, which depends on local conditions. This is important because some fraction of the internal heating will be highly inhomogeneous, occurring predominantly in compressions and shocks as gas enters a high density spiral structure, or at high altitudes where waves from the interior are refracted and steepen into shocks (*Pickett et al.* 2000a) and where disks may be irradiated (*Mejía*, 2004; *Cai et al.*, 2006). Temperatures and the $t_{cool}$'s that depend on them will then be neither simple functions of radius, nor a single globally defined value. Depending on whether the local cooling time of the gas inside the high density spiral structure is short enough, fragmentation will be more or less likely, and additional hydrodynamic processes such as convection may become active if large enough gradients can be generated.

Indeed, recent simulations of *Boss* (2002a, 2004a) suggest that vertical convection is active in disks when radiative transfer is included, as expected for high $\tau$ according to *Ruden and Pollack* (1991). This is important because convection will keep the upper layers of the disk hot, at the expense of the dense interior, so that radiative cooling is more efficient and fragmentation is enhanced. The results have not yet been confirmed by other work and therefore remain somewhat controversial. Simulations by *Mejía* (2004) and *Cai et al.* (2006) are most similar to those of *Boss* and could have developed convection sufficient to induce fragmentation, but none seems to occur. No fragmentation occurs in *Nelson et al.* (2000) either, where convection is implicitly assumed to be efficient through their assumption that the entropy of each vertical column is constant. Recent re-analysis of their results reveals $t_{cool} \sim 3$ to 10 $P_{rot}$, depending on radius, which is too long to allow fragmentation. These $t_{cool}$'s are in agreement with those seen by *Cai et al.* (2006) and by *Mejía et al.* (in preparation) for solar metallicity. The *Nelson et al.* results are also interesting because their comparison of the radiated output to SEDs observed for real systems demonstrates that substantial additional heating beyond that supplied by GI's is required to reproduce the observations, perhaps further inhibiting fragmentation in their models. However, using the same temperature distribution between 1 and 10 AU now used in Boss's GI models, combined with temperatures outside this region taken from models by *Adams et al.* (1988), *Boss and Yorke* (1996) are able to reproduce the SED of the T Tauri system. It is unclear at present why their results differ from those of *Nelson et al.* (2000).

The origins of the differences between the three studies are uncertain, but possibilities include differences of both numerical and physical origin. The boundary treatment at the optically thick/thin interface is different in each case (see Section 3.2), influencing the efficiency of cooling, as are the numerical methods and resolutions. *Boss* and the *Cai/Mejía* group each use 3D grid codes but with spherical and cylindrical grids respectively, and each with a different distribution of grid zones, while *Nelson et al.* use a 2D SPH code. Perhaps significantly, *Cai/Mejía* assume their ideal gas has $\gamma = 5/3$ while *Boss* adopts an EOS that includes rotational and vibrational states of hydrogen, so that $\gamma \approx 7/5$ for typical disk conditions. It is possible that differences in the current results may be explained if the same sensitivities to $\gamma$ seen in fixed EOS and fixed cooling simulations also hold when radiative transfer is included. *Boss and Cai* (in preparation) are now conducting direct comparison calculations to isolate the cause of their differences. The preliminary indication is that the radiative boundary conditions may be the critical factor.

Discrepant results for radiatively cooled models should not overshadow the qualitative agreement reached about the relationship between disk thermodynamics and fragmenta-

tion. If the marginally unstable state of a self-regulated disk is upset quickly enough by an increase in cooling or decrease in heating, the disk may fragment. What is still very unclear is whether such conditions can develop in real planet-forming disks. It is key to develop a full 3D portrait of the disk surface, so that radiative heating and cooling sources may be included self-consistently in numerical models. Important heating sources will include the envelope, the central star, neighboring stars, and self-heating from other parts of the disk, all of which will be sensitive to shadowing caused by corrugations in the disk surface that develop and change with time due to the GI's themselves. Preliminary studies of 3D disk structure (*Boley and Durisen*, 2006) demonstrate that vertical distortions, analogous to hydraulic jumps, will in fact develop (see also *Pickett et al.*, 2003). If these corrugations are sufficient to cause portions of the disk to be shadowed, locally rapid cooling may occur in the shadowed region, perhaps inducing fragmentation.

An implicit assumption of the discussion above is that the opacity is well known. In fact, it is not. The dominant source of opacity is dust, whose size distribution, composition, and spatial distribution will vary with time (*Cuzzi et al.*, 2001; *Klahr*, 2003, see also Section 5 below), causing the opacity to vary as a result. So far, no models of GI evolution have included effects from any of these processes, except that *Nelson et al.* model dust destruction while *Cai* and *Mejía* consider opacity due to large grains. Possible consequences are a misidentification of the disk photospheric surface if dust grains settle towards the midplane, or incorrect radiative transfer rates in optically thick regions if the opacities themselves are in error.

### 4.3 Orbital Survival of Clumps

Once dense clumps form in a gravitationally unstable disk, the question becomes one of survival: Are they transient structures or permanent precursors of giant planets? Long-term evolution of simulations that develop clumps is difficult because it requires careful consideration of not only the large-scale dynamical processes that dominate formation but also physical processes that exert small influences over long time scales (e.g., migration and transport due to viscosity). It also requires that boundary conditions be handled gracefully in cases where a clump or the disk itself tries to move outside the original computational volume.

On a more practical level, the extreme computational cost of performing such calculations limits the time over which systems may be simulated. As a dense clump forms, the temperatures, densities, and fluid velocities within it all increase. As a result, time steps, limited by the Courant condition, can decrease to as little as minutes or hours as the simulation attempts to resolve the clump's internal structure. So far only relatively short integration times of up to a few$\times 10^3$ yrs have been possible. Here, we will focus on the results of simulations and refer the reader to the chapters by *Papaloizou et al.* and *Levison et al.* for discussions of longer-term interactions.

In the simplest picture of protoplanet formation via GI's, structures are assumed to evolve along a continuum of states that are progressively more susceptible to fragmentation, presumably ending in one or more bound objects which eventually become protoplanets. *Pickett et al.* (1998, 2000a, 2003) and *Mejía et al.* (2005) simulate initially smooth disks subject to growth of instabilities and, indeed, find growth of large-amplitude spiral structures that later fragment into arclets or clumps. Instead of growing more and more bound, however, these dense structures are sheared apart by the background flow within an orbit or less, especially when shock heating is included via an artificial viscosity. This suggests that a detailed understanding of the thermodynamics inside and outside the fragments is critical for understanding whether fragmentation results in permanently bound objects.

Assuming that permanently bound objects do form, two additional questions emerge. First, how do they accrete mass and how much do they accrete? Second, how are they influenced by the remaining disk material? Recently, *Mayer et al.* (2002, 2004a) and *Lufkin et al.* (2004) have used SPH calculations to follow the formation and evolution of clumps in simulations covering up to 50 orbits (roughly 600 yrs), and *Mayer et al.* (in preparation) are extending these calculations to several thousand years. They find that, when a locally isothermal EOS is used well past initial fragmentation, clumps grow to $\sim 10 M_J$ within a few hundred years. On the other hand, in simulations using an ideal gas EOS plus bulk viscosity, accretion rates are much lower ($< 10^{-6} M_\odot$/yr), and clumps do not grow to more than a few $M_J$ or $\sim 1\%$ of the disk mass. The assumed thermodynamic treatment has important effects not only on the survival of clumps, but also on their growth.

*Nelson and Benz* (2003), using a grid-based code and starting from a $0.3 M_J$ seed planet, show that accretion rates this fast are unphysically high because the newly accreted gas cannot cool fast enough, even with the help of convection, unless some localized dynamical instability is present in the clump's envelope. So, the growth rate of an initially small protoplanet may be limited by its ability to accept additional matter rather than the disk's ability to supply it. They note (see also *Lin and Papaloizou*, 1993; *Bryden et al.*, 1999; *Kley*, 1999; *Lubow et al.*, 1999; *Nelson et al.*, 2000) that the accretion process after formation is self-limiting at a mass comparable to the largest planet masses yet discovered (see the chapter by *Udry et al.*).

Fig. 4 shows one of the extended *Mayer et al.* simulations, containing two clumps in one disk realized with $2 \times 10^5$ particles, and run for about 5,000 years (almost 200 orbits at 10 AU). There is little hint of inward orbital migration over a few thousand year time scale. Instead, both clumps appear to migrate slowly outward. *Boss* (2005) uses sink particles ("virtual planets") to follow a clumpy disk for about 1,000 years. He also finds that the clumps do not migrate rapidly. In both works, the total simulation times are quite short compared to the disk lifetime and so are only

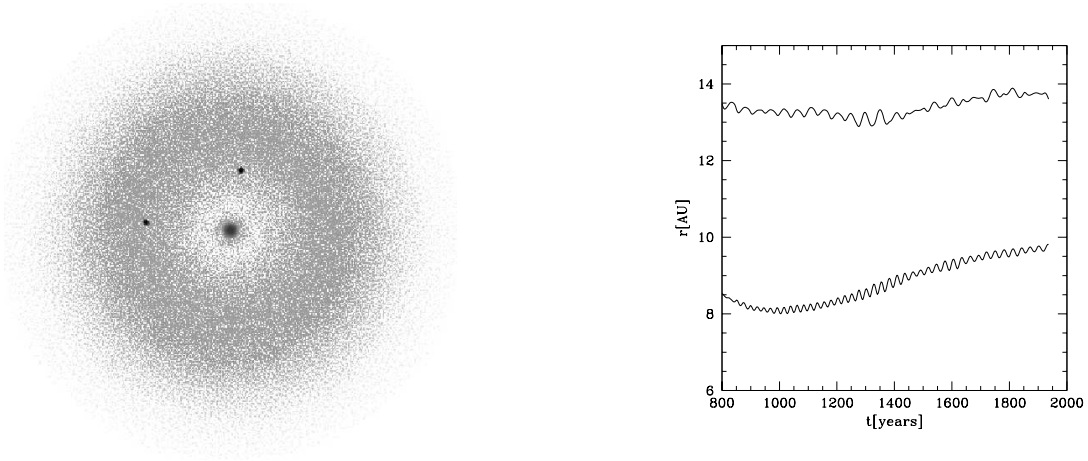


Fig. 4.— The orbital evolution of two clumps (right) formed in a massive, growing protoplanetary disk simulation described in Mayer et al. (2004). A face-on view of the system after 2264 years of evolution is shown on the left, using a color coded density map (the box is 38 AU on a side). In the right panel, the orbital evolution of the two clumps is shown. Overal, both clumps migrate outward.

suggestive of the longer-term fate of the objects. Nevertheless, the results are important, because they illustrate shortcomings in current analytic models of migration.

Although migration theory is now extremely well developed (see the chapter by *Papaloizou et al.*), predictions for migration at the earliest phases of protoplanet formation by GI's are difficult to make, because many of the assumptions on which the theory is based are not well satisfied. More than one protoplanet may form in the same disk, they may form with masses larger than linear theory can accommodate, and they may be significantly extended rather than the point masses assumed by theory. If the disk remains massive, it may also undergo gravitoturbulence that changes the disk's mass distribution on a short enough time scale to call into question the resonance approximations in the theory. If applicable in the context of these limitations, recent investigations into the character of corotation resonances (see the chapter by *Papaloizou et al.*) and vortex excitation (*Koller et al.*, 2003) in the corotation region may be of particular interest, because a natural consequence of these processes is significant mass transport across the clump's orbit and reduced inward migration, which is in fact seen in the above simulations.

### 4.4 Comparison Test Cases

Disk instability has been studied so far with various types of grid codes and SPH codes that have different relative strengths and weaknesses (Section 3). Whether different numerical techniques find comparable results with nearly identical assumptions is not yet known, although some comparative studies have been attempted (*Nelson et al.*, 1998). Several aspects of GI behavior can be highly dependent on code type. For example, SPH codes require artificial viscosity to handle shocks such as those occurring along spiral arms. Numerical viscosity can smooth out the velocity field in overdense regions, possibly inhibiting collapse (*Mayer et al.*, 2004a) but, at the same time, possibly increasing clump longevity if clumps form (see Fig. 3 of *Durisen*, 2006). Gravity solvers that are both accurate and fast are a robust feature of SPH codes, while gravity solvers in grid codes can under-resolve the local self-gravity of the gas (*Pickett et al.*, 2003). Both types of codes can lead to spurious fragmentation or suppress it when a force imbalance between pressure and gravity results at scales comparable to the local Jeans or Toomre length due to lack of resolution (*Truelove et al.*, 1997; *Bate and Burkert*, 1997; *Nelson*, 2006).

Another major code difference is in the set up of initial conditions. Although both Eulerian grid-based and Lagrangian particle-based techniques represent an approximation to the continuum fluid limit, noise levels due to discreteness are typically higher in SPH simulations. Initial perturbations are often applied in grid-based simulations to seed GI's (either random or specific modes or both, e.g., *Boss*, 1998a), but are not required in SPH simulations, because they already have built-in Poissonian noise at the level of $\sqrt{N}/N$ or more, where $N$ is the number of particles. In addition, the SPH calculation of hydrodynamic variables introduces small scale noise at the level of $1/N_{neigh}$, where $N_{neigh}$ is the number of neighboring particles contained in one smoothing kernel. Grid-based simulations require boundary conditions which restrict the dynamic range of the simulations. For example, clumps may reach the edge of a computational volume after only a limited number of orbits (*Boss*, 1998a, 2000; *Pickett et al.*, 2000a). Cartesian grids can lead to artificial diffusion of angular momentum in a disk, a problem that can be avoided using a cylindrical grid (*Pickett et al.*, 2000a) or spherical grid (*Boss and Myhill*, 1992). *Myhill & Boss* (1993) find good agreement between spherical and Cartesian grid results for a nonisothermal rotating protostellar collapse problem, but evolution of a nearly equilibrium disk over many orbits in a Cartesian grid is probably still a challenge.

In order to understand how well different numerical tech-

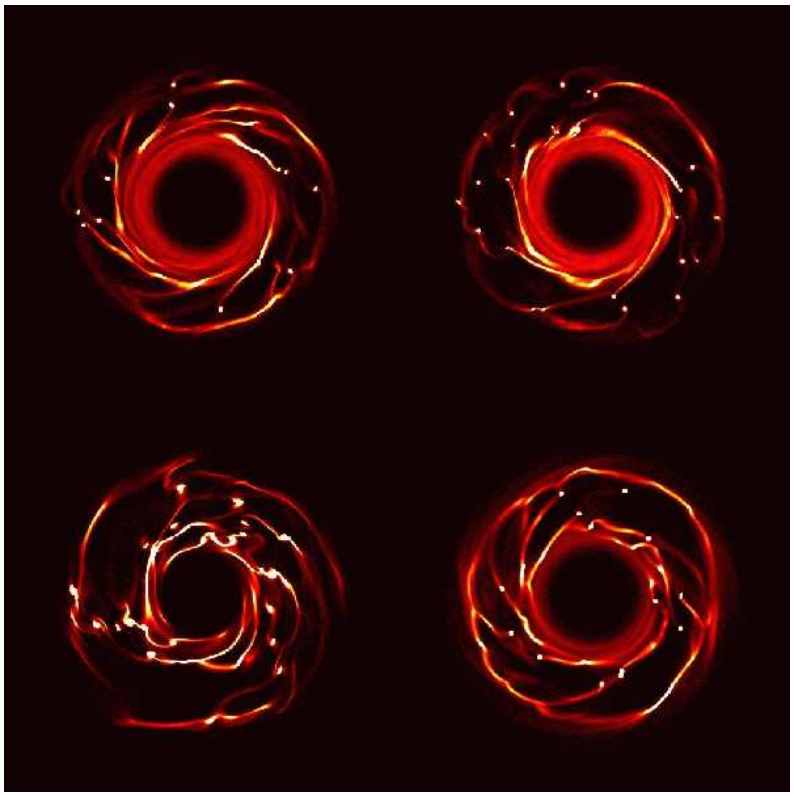

Fig. 5.— Equatorial slice density maps of the disk in the test runs after about 100 yrs of evolution. The initial disk is 20 AU in diameter. From top left to bottom right are the results from GASOLINE and GADGET2 (both SPH codes), from the Indiana cylindrical-grid code, and from the AMR Cartesian-grid code FLASH. The SPH codes adopt the shear-reduced artificial viscosity of *Balsara* (1995).

niques can agree on the outcome of GI's, different codes need to run the same initial conditions. This is being done in a large, on-going code-comparison project that involves eight different codes, both grid-based and SPH. Among the grid codes, there are several adaptive mesh refinement (AMR) schemes. The comparison is part of a larger effort involving several areas of computational astrophysics (http://krone.physik.unizh.ch/∼moore/wengen/tests.html). The system chosen for the comparison is a uniform temperature, massive, and initially very unstable disk with a diameter of about 20 AU. The disk is evolved isothermally and has a $Q$ profile that decreases outward, reaching a minimum value $\sim 1$ at the disk edge. The disk model is created using a particle representation by letting its mass grow slowly, as described in *Mayer et al.* (2004a). This distribution is then interpolated onto the various grids.

Here we present the preliminary results of the code comparisons from four codes – two SPH codes called GASOLINE (*Wadsley et al.*, 2004) and GADGET2 (*Springel et al.*, 2001; *Springel*, 2005), the Indiana University code with a fixed cylindrical grid (*Pickett*, 1995; *Mejía*, 2004), and the Cartesian AMR code called FLASH (*Fryxell et al.*, 2000). Readers should consult the published literature for detailed descriptions, but we briefly enumerate some basic features. FLASH uses a PPM-based Riemann solver on a Cartesian grid with directional splitting to solve the Euler equations, and it uses an iterative multi-grid Poisson solver for gravity. Both GASOLINE and GADGET2 solve the Euler equations using SPH and solve gravity using a treecode, a binary tree in the case of GASOLINE and an oct-tree in the case of GADGET2. Gravitational forces from individual particles are smoothed using a spline kernel softening, and they both adopt the *Balsara* (1995) artificial viscosity that minimizes shear forces on large scales. The Indiana code is a finite difference grid-based code which solves the equations of hydrodynamics using the Van Leer method. Poisson's equation is solved at the end of each hydrodynamic step by a Fourier transform of the density in the azimuthal direction, direct solution by cyclic reduction of the transform in ($r$,$z$), and a transform back to real space (*Tohline*, 1980). The code's Von Neumann-Richtmeyer artificial bulk viscosity is not used for isothermal evolutions.

The two SPH codes are run with fixed gravitational softening, and the local Jeans length (see *Bate and Burkert*, 1997) before and after clump formation is well resolved. Runs with adaptive gravitational softening will soon be included in the comparison. Here we show the results of the runs whose initial conditions were generated from the $8 \times 10^5$ particles setup, which was mapped onto a 512x512x52 Cartesian grid for FLASH and onto a 512x1024x64 ($r$,$\phi$,$z$) cylindrical grid for the Indiana code. Comparable resolution (cells for grids or gravity softening for SPH runs) is available initially in the outer part of the disk, where the Q parameter reaches its minimum. In the GASOLINE and

GADGET2 runs, the maximum spatial resolution is set by the gravitational softening at 0.12 AU. Below this scale, gravity is essentially suppressed. The FLASH run has a initial resolution of 0.12 AU at 10 AU, comparable with the SPH runs. The Indiana code has the same resolution as FLASH in the radial direction but has a higher azimuthal resolution of 0.06 AU at 10 AU.

As it can be seen from Fig. 5, the level of agreement between the runs is satisfactory, although significant differences are noticeable. More clumps are seen in the Indiana code simulation. On the other end, clumps have similar densities in FLASH and GASOLINE, while they appear more fluffy in the Indiana code than in the other three. The causes are probably different gravity solvers and the non-adaptive nature of the Indiana code. Even within a single category of code, SPH or grid-based, different types of viscosity, both artificial and numerical, might be more or less diffusive and affect the formation and survival of clumps. In fact, tests show that more fragments are present in SPH runs with shear-reduced artificial viscosity than with full shear viscosity.

Although still in an early stage, the code comparison has already produced one important result, namely that, once favorable conditions exist, widespread fragmentation is obtained in high-resolution simulations using any of the standard numerical techniques. On the other hand, the differences already noticed require further understanding and will be addressed in a forthcoming paper (*Mayer et al.*, in preparation). Although researchers now agree on conditions for disk fragmentation, no consensus yet exists about whether or where real disks fragment or how long fragments really persist. Answers to these questions require advances over current techniques for treating radiative physics and compact structures in global simulations.

## 5. INTERACTIONS WITH SOLIDS

The standard model for the formation of giant gaseous planets involves the initial growth of a rocky core that, when sufficiently massive, accretes a gaseous envelope (*Bodenheimer and Pollack*, 1986; *Pollack et al.*, 1996). In this scenario, the solid particles in the disk must first grow from micron-sized dust grains to kilometer-sized planetesimals that then coagulate to form the rocky core.

In a standard protoplanetary disk, the gas pressure near the disk midplane will generally decrease with increasing radius resulting in an outward pressure gradient that causes the gas to orbit with sub-Keplerian velocities. The solid particles, on the other hand, do not feel the gas pressure and orbit with Keplerian velocities. This velocity difference results in a drag force that generally causes the solid particles to lose angular momentum and to spiral inward toward the central star with a radial drift velocity that depends on the particle size (*Weidenschilling*, 1977).

While this differential radial drift can mix together particles of different size and allow large grains to grow by sweeping up smaller grains (*Weidenschilling and Cuzzi*, 1993), it also introduces a potential problem. Depending on the actual disk properties, the inward radial velocity for particles with sizes between 1 cm and 1 m can be as high as $10^4$ cm s$^{-1}$ (*Weidenschilling*, 1977), so that these particles could easily migrate into the central star before becoming large enough to decouple from the disk gas. If these particles do indeed have short residence times in the disk, it is difficult to envisage how they can grow to form the larger kilometer-sized planetesimals which are required for the subsequent formation of the planetary cores.

The above situation is only strictly valid in smooth, laminar disks with gas pressures that decrease monotonically with increasing radius. If there are any regions in the disk that have local pressure enhancements, the situation can be very different. In the vicinity of a pressure enhancement, the gas velocity can be either super- and sub-Keplerian depending on the local gas pressure gradient. The drag force can then cause solid particles to drift outwards or inwards, respectively (*Haghighipour and Boss*, 2003a,b). The net effect is that the solid particles should drift towards pressure maxima. A related idea is that a baroclinic instability could lead to the production of long-lived, coherent vortices (*Klahr and Bodenheimer*, 2003) and that solid particles would drift towards the center of the vortex where the enhanced concentration could lead to accelerated grain growth (*Klahr and Henning*, 1997). The existence of such vortices is, however, uncertain (*Johnson and Gammie*, 2006).

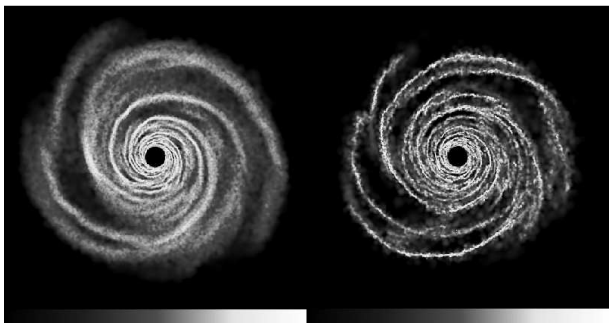

Fig. 6.— Surface density structure of particles embedded in a self-gravitating gas disk. a) The left-hand panel shows that the distribution of 10 m radius particles is similar to that of the gas disk, because these particles are not influenced strongly by gas drag. b) The right-hand panel illustrates that 50 cm particles are strongly influenced by gas drag and become concentrated into the GI-spirals with density enhancements of an order of magnitude or more. Figures adapted from *Rice et al.* (2004).

An analogous process could occur in a self-gravitating disk, where structures formed by GI activity, such as the centers of the spiral arms, are pressure and density maxima. In such a case, drag force results in solid particles drifting towards the centers of these structures, with the most significant effect occurring for those particles that would, in a smooth, laminar disk, have the largest inward radial velocities.

If disks around very young protostars do indeed undergo a self-gravitating phase, then we would expect the resulting

spiral structures to influence the evolution of the solid particles in the disk (*Haghighipour and Boss*, 2003a,b). A GI-active disk will also transport dust grains small enough to remain tied to the gas across distances of many AU's in only 1,000 yrs or so (*Boss*, 2004b), a potentially important process for explaining the components of primitive meteorites (see the chapter by *Alexander et al.*). *Boley and Durisen* (2006) show that, in only one pass of a spiral shock, hydraulic jumps induced by shock heating can mix gas and entrained dust radially and vertically over length-scales $\sim H$ through the generation of huge breaking waves. The presence of chondrules in primitive chondritic meteorites is circumstantial evidence that the Solar Nebula experienced a self-gravitating phase in which spiral shock waves provided the flash heating required to explain their existence (*Boss and Durisen*, 2005a,b; *Boley et al.*, 2005).

To test how a self-gravitating phase in a protostellar disk influences the evolution of embedded particles, *Rice et al.* (2004) perform 3D self-gravitating disk simulations that include particles evolved under the influence of both disk self-gravity and gas drag. In their simulations, they consider both 10 m particles, which, for the chosen disk parameters, are only weakly coupled to the gas, and 50 cm particles that are significantly influenced by the gas drag. Fig. 6a shows the surface density structure of the 10 m particles one outer rotation period after they were introduced into the gas disk. The structure in the particle disk matches closely that of the gas disk (not shown) showing that these particles are influenced by the gravitational force of the gas disk, but not so strongly influenced by gas drag. Fig. 6b shows the surface density structure of 50 cm particles at the same epoch. Particles of this size are influenced by gas drag and Fig. 6b shows that, compared to the 10 m particles, these particles become strongly concentrated into the GI-induced spiral structures.

The ability of solid particles to become concentrated in the center of GI-induced structures suggests that, even if giant planets do not form directly via GI's, a self-gravitating phase may still play an important role in giant planet formation. The solid particles may achieve densities that could accelerate grain growth either through an enhanced collision rate or through direct gravitational collapse of the particle sub-disk (*Youdin and Shu*, 2002). *Durisen et al.* (2005) also note that dense rings can be formed near the boundaries between GI-active and inactive regions of a disk (e.g., the central disk in Fig. 1). Such rings are ideal sites for the concentration of solid particles by gas drag, possibly leading to accelerated growth of planetary embryos. Even if processes like these do not contribute directly to planetesimal growth, GI's may act to prevent the loss of solids by migration toward the proto-Sun. The complex and time-variable structure of GI activity should increase the residence time of solids in the disk and potentially give them enough time to become sufficiently massive to decouple from the disk gas.

## 6. PLANET FORMATION

The relatively high frequency ($\sim$10%) of solar-type stars with giant planets that have orbital periods less than a few years suggests that longer-period planets may be quite frequent. Perhaps $\sim$ 12 to 25% of G dwarfs may have gas giants orbiting within $\sim$10 AU. If so, gas giant planet formation must be a fairly efficient process. Because roughly half of protoplanetary disks disappear within 3 Myr or less (*Bally et al.*, 1998; *Haisch et al.*, 2001; *Bricẽno et al.*, 2001; *Eisner and Carpenter*, 2003), core accretion may not be able to produce a high frequency of gas giants. There is also now strong theoretical (*Yorke and Bodenheimer*, 1999) and observational (*Osorio et al.*, 2003; *Rodríguez et al.*, 2005; *Eisner et al.*, 2005) evidence that disks around very young protostars should indeed be sufficiently massive to experience GI's. *Rodríguez et al.* (2005) show a 7 mm VLA image of a disk around a Class 0 protostar that may have a mass half that of the central star.

Hybrid scenarios may help remove the bottleneck by concentrating meter-sized solids, but it is not clear that they can shorten the overall time scale for core accretion, which is limited by the time needed for the growth of 10 $M_\oplus$ cores and for accretion of a large gaseous envelope. *Durisen et al.* (2005) suggest that the latter might be possible in dense rings, but detailed calculations of core growth or envelope accretion in the environment of a dense ring do not now exist. Disk instability, on the other hand, has no problem forming gas giants rapidly in even the shortest-lived protoplanetary disk. Most stars form in regions of high-mass star formation (*Lada and Lada*, 2003) where disk lifetimes should be the shortest due to loss of outer disk gas by UV irradiation.

There is currently disagreement about whether GI's are stronger in low-metallicity systems (*Cai et al.*, 2006) or whether their strength is relatively insensitive to the opacity of the disk (*Boss*, 2002a). In either case, if disk instability is correct, we would expect that even low-metallicity stars could host gas giant planets. The growth of cores in the core accretion mechanism is hastened by higher metallicity through the increase in surface density of solids (*Pollack et al.*, 1996), although the increased envelope opacity, which slows the collapse of the atmosphere, works in the other direction (*Podolak*, 2003). The recent observation of a Saturn mass object, orbiting the metal-rich star HD 149026, with a core mass equal to approximately half the planet's mass (*Sato et al.*, 2005) has been suggested as a strong confirmation of the core accretion model. It has, however, yet to be shown that the core accretion model can produce a core with such a relatively large mass. If this core was produced by core accretion, it seems that it never achieved a runaway growth of its envelope; yet, in the case of Jupiter, the core accretion scenario requires efficient accumulation of a massive envelope around a relatively low-mass core.

The correlation of short-period gas giants with high metallicity stars is often interpreted as strong evidence in favor of core accretion (*Laws et al.*, 2003; *Fischer et al.*,

2004; *Santos et al.*, 2004). The *Santos et al.* (2004) analysis, however, shows that even the stars with the lowest metallicities have detectable planets with a frequency comparable to or higher than that of the stars with intermediate metallicities. *Rice et al.* (2003c) have shown that the metallicity distribution of systems with at least one massive planet ($M_{pl} > 5M_{Jup}$) on an eccentric orbits of moderate semi-major axis does not have the same metal-rich nature as the full sample of extrasolar planetary systems. Some of the metallicity correlation can be explained by the observational bias of the spectroscopic method in favor of detecting planets orbiting stars with strong metallic absorption lines. The residual velocity jitter typically increases from a few m/s for solar metallicity to 5 – 16 m/s for stars with 1/4 the solar metallicity or less. In terms of extrasolar planet search space, this could account for as much as a factor of two difference in the total number of planets detected by spectroscopy. A spectroscopic search of 98 stars in the Hyades cluster, with a metallicity 35% greater than solar, found nothing, whereas about 10 hot Jupiters should have been found, assuming the same frequency as in the solar neighborhood (*Paulson et al.*, 2004).

*Jones* (2004) found that the average metallicity of planet-host stars increased from $\sim 0.07$ to $\sim 0.24$ dex for planets with semimajor axes of $\sim 2$ AU to $\sim 0.03$ AU, suggesting a trend toward shortest-period planets orbiting the most metal-rich stars. Similarly, *Sozzetti* (2004) showed that both metal-poor and metal-rich stars have increasing numbers of planets as the orbital period increases but only the metal-rich stars have an excess of the shortest period planets. This could imply that the metallicity correlation is caused by inward orbital migration, if low-metallicity stars have long-period giant planets that seldom migrate inward.

Lower disk metallicity results in slower Type II inward migration (*Livio and Pringle*, 2003), the likely dominant mechanism for planet migration (see the chapter by *Papaloizou et al.*). This is because with increased metallicity, the disk viscosity $\nu$ increases. In standard viscous accretion disk theory (e.g., *Ruden and Pollack*, 1991) $\nu = \alpha c_s H$. Lower disk metallicity leads to lower disk opacity, lower disk temperatures, lower sound speeds, and a thinner disk. As $\nu$ decreases with lowered metallicity, the time scale for Type II migration increases. *Ruden and Pollack* (1991) found that viscous disk evolution times increased by a factor of about 20 when $\nu$ decreased by a factor of 10. It remains to be seen if this effect is large enough to explain the rest of the correlation. If disk instability is operative and if orbital migration is the major source of the metallicity correlation, then metal-poor stars should have planets on long-period orbits.

Disk instability may be necessary to account for the long-period giant planet in the M4 globular cluster (*Sigurdsson et al.*, 2003), where the metallicity is 1/20 to 1/30 solar metallicity. The absence of short-period Jupiters in the 47 Tuc globular cluster (*Gilliland et al.*, 2000) with 1/5 solar metallicity could be explained by the slow rate of inward migration due to the low metallicity. Furthermore, if 47 Tuc initially contained OB stars, photoevaporation of the outer disks may have occurred prior to inward orbital migration of any giant planets, preventing their evolution into short-period planets, though other factors (i.e., crowding) can also be important in these clusters.

The M dwarf GJ 876 is orbited by a pair of gas giants (as well as a much smaller mass planet) and other M dwarfs have giant planets as well (*Butler et al.*, 2004), though apparently not as frequently as the G dwarfs. *Laughlin et al.* (2004) found that core accretion was too slow to form gas giants around M dwarfs because of the longer orbital periods. Disk instability does not a have similar problem for M dwarfs, and disk instability predicts that M, L, and T dwarfs should have giant planets.

With disk instability, one Jupiter mass of disk gas has at most $\sim 6M_{\oplus}$ of elements suitable to form a rock/ice core. The preferred models of the Jovian interior imply that Jupiter's core mass is less than $\sim 3M_{\oplus}$ (*Saumon and Guillot*, 2004); Jupiter may even have no core at all. These models seem to be consistent with formation by disk instability and inconsistent with formation by core accretion, which requires a more massive core. As a result, the possibility of core erosion has been raised (*Saumon and Guillot*, 2004). If core erosion can occur, core masses may lose much of their usefulness as formation constraints. Saturn's core mass appears to be larger than that of Jupiter (*Saumon and Guillot*, 2004), perhaps $\sim 15M_{\oplus}$, in spite of it being the smaller gas giant. Core erosion would only make Saturn's initial core even larger. Disk instability can explain the larger Saturnian core mass (*Boss et al.*, 2002). Proto-Saturn may have started out with a mass larger than that of proto-Jupiter, but its excess gas may have been lost by UV photoevaporation, a process that could also form Uranus and Neptune. Disk instability predicts that inner gas giants should be accompanied by outer ice giant planets in systems which formed in OB associations due to strong UV photoevaporation. In low-mass star-forming regions, disk instability should produce only gas giants, without outer ice giants.

Disk instability predicts that even the youngest stars should show evidence of gas giant planets (*Boss*, 1998b), whereas core accretion requires several Myr or more to form gas giants (*Inaba et al.*, 2003). A gas giant planet seems to be orbiting at $\sim 10$ AU around the 1 Myr-old star CoKu Tau/4 (*Forrest et al.*, 2004), based on a spectral energy distribution showing an absence of disk dust inside 10 AU (for an alternative perspective, see *Tanaka et al.*, 2005). Several other 1 Myr-old stars show similar evidence for rapid formation of gas giant planets. The direct detection of a possible gas giant planet around the 1 Myr-old star GQ Lup (*Neuhäuser et al.*, 2005) similarly requires a rapid planet formation process.

We conclude that there are significant observational arguments to support the idea that disk instability, or perhaps a hybrid theory where core accretion is accelerated by GI's, might be required to form some if not all gas giant planets. Given the major uncertainties in the theories, observational tests will be crucial for determining the relative proportions

of giant planets produced by the competing mechanisms.

**Acknowledgments.** R.H.D.'s contribution was supported by NASA grants NAG5-11964 and NNG05GN11G and A.P.B.'s by NASA grants NNG05GH30G, NNG05GL10G, and NCC2-1056. Support for A.F.N. was provided by the U.S. Department of Energy under contract W-7405-ENG-36, for which this is publication LA-UR–05-7851. We would like to thank S. Michael for invaluable assistance in manuscript preparation, an anonymous referee for substantive improvements, and A.C. Mejía, A. Gawryszczak, and V. Springel for allowing us to premier their comparison calculations in Section 4.4. FLASH was in part developed by the DOE-supported ASC/Alliance Center for Astrophysical Thermonuclear Flashes at the University of Chicago and was run on computers at Warsaw's Interdisciplinary Center for Mathematical and Computational Modeling.

REFERENCES

Adams F. C., Shu F. H., and Lada C. J. (1988) *Astrophys. J., 326*, 865-883.

Adams F. C., Ruden S. P., and Shu F. H. (1989) *Astrophys. J., 347*, 959-976.

Armitage P. J., Livio M., and Pringle J. E. (2001) *Mon. Not. R. Astron. Soc., 324*, 705-711.

Balbus S. A. and Papaloizou J. C. B. (1999) *Astrophys. J., 521*, 650-658.

Balsara D. S. (1995) *J. Comput. Phys., 121*, 357-372.

Bate M. R. and Burkert A. (1997) *Mon. Not. R. Astron. Soc., 228*, 1060-1072.

Bally J., Testi L., Sargent A., and Carlstrom J. (1998) *Astron. J., 116*, 854-859.

Beckwith S. V. W., Sargent A. I., Chini R. S., and Güsten R. (1990) *Astron. J., 99*, 924-945.

Benz W. (1990) In *The Numerical Modeling of Nonlinear Stellar Pulsations* (J. R. Buchler, ed.), pp. 269-288. Kluwer, Boston.

Boffin H. M. J., Watkins S. J., Bhattal A. S., Francis N., and Whitworth A. P. (1998) *Mon. Not. R. Astron. Soc., 300*, 1189-1204.

Bodenheimer P. and Pollack J. B. (1986) *Icarus, 67*, 391-408.

Bodenheimer P., Yorke H. W., Różyczka M., and Tohline J. E. (1990) *Astrophys. J., 355*, 651-660.

Boley A. C. and Durisen R. H. (2006) *Astrophys. J.*, in press (astro-ph 0510305).

Boley A. C., Durisen R. H., and Pickett M. K. (2005) In *Chondrites and the Protoplanetary Disk* (A. N. Krot et al., eds.), pp. 839-848. ASP Conference Series, San Francisco.

Boss A. P. (1997) *Science, 276*, 1836-1839.

Boss A. P. (1998a) *Astrophys. J., 503*, 923-937.

Boss A. P. (1998b) *Nature, 395*, 141-143.

Boss A. P. (2000) *Astrophys. J., 536*, L101-L104.

Boss A. P. (2001) *Astrophys. J., 563*, 367-373.

Boss A. P. (2002a) *Astrophys. J., 567*, L149-L153.

Boss A. P. (2002b) *Astrophys. J., 576*, 462-472.

Boss A. P. (2002c) *Earth Planet. Sci. Let., 202*, 513-523.

Boss A. P. (2003) *Lunar Planet. Inst., 34*, 1075-1076.

Boss, A. P. (2004a) *Astrophys. J., 610*, 456-463.

Boss A. P. (2004b) *Astrophys. J., 616*, 1265-1277.

Boss A. P. (2005) *Astrophys. J., 629*, 535-548.

Boss A. P. (2006) *Astrophys. J.*, in press.

Boss A. P. and Durisen R. H. (2005a) *Astrophys. J., 621*, L137-L140.

Boss A. P. and Durisen R. H. (2005b) In *Chondrites and the Protoplanetary Disk* (A. N. Krot et al., eds.), pp. 821-838. ASP Conference Series, San Francisco.

Boss A. P. and Myhill E. A. (1992) *Astrophys. J. Suppl., 83*, 311-327.

Boss A. P. and Yorke H. W. (1996) *Astrophys. J., 496*, 366-372.

Boss A. P., Wetherill G. W., and Haghighipour N. (2002) *Icarus, 156*, 291-295.

Briceño C., Vivas A. K., Calvet N., Hartmann L., Pachecci R. et al. (2001) *Science, 291*, 93-96.

Butler R. P., Vogt S. S., Marcy G. W., Fischer D. A., Wright J. T. et al. (2004) *Astrophys. J., 617*, 580-588.

Bryden G., Lin D. N. C., and Ida S. (2000) *Astrophys. J., 544*, 481-495.

Cai K., Durisen R. H., Michael S., Boley A. C., Mejía A. C., Pickett M. K., and D'Alessio P. (2006) *Astrophys. J., 636*, L149-L152.

Cameron A. G. W. (1978) *Moon Planets, 18*, 5-40.

Chiang E. I. and Goldreich P. (1997) *Astrophys. J., 490*, 368-376.

Colella P. and Woodward P. R. (1984) *J. Comp. Phys., 54*, 174-201.

Cuzzi J. N., Hogan R. C., Paque J. M., and Dobrovolskis A. R. (2001) *Astrophys. J., 546*, 496-508.

D'Alessio P., Calvet N., and Hartmann L. (1997) *Astrophys. J., 474*, 397-406.

D'Alessio P., Cantó J., Calvet N., and Lizano S. (1998) *Astrophys. J., 500*, 411-427.

Durisen R. H. (2006) In *A Decade of Extrasolar Planets Around Normal Stars* (M. Livio, ed.), in press. University Press, Cambridge.

Durisen R. H., Cai K., Mejía A. C., and Pickett M. K. (2005) *Icarus, 173*, 417-424.

Durisen R. H., Mejía A. C., and Pickett B. K. (2003) *Rec. Devel. Astrophys., 1*, 173-201.

Durisen R. H., Mejía A. C., Pickett B. K., and Hartquist T. W. (2001) *Astrophys. J., 563*, L157-L160.

Eisner J. A. and Carpenter J. M. (2003) *Astrophys. J., 598*, 1341-1349.

Eisner J. A., Hillenbrand L. A., Carpenter J. M., and Wolf S. (2005) *Astrophys. J., 635*, 396-421.

Fischer D., Valenti J. A. and Marcy G. (2004) In *IAU Symposium #219: Stars as Suns: Activity, Evolution, and Planets* (A. K. Dupree and A. O. Benz, eds.), pp. 29-38. APS Conference Series, San Francisco.

Forrest W. J., Sargent B., Furlan E., D'Alessio P., Calvet N. et al. (2004) *Astrophys. J. Suppl., 154*, 443-447.

Fleming T. and Stone J. M. (2003) *Astrophys. J., 585*, 908-920.

Fryxell B., Arnett D., and Müller E. (1991) *Astrophys. J., 367*, 619-634.

Fryxell B., Olson K., Ricker P., Timmes F. X., Zingale M. et al. (2000) *Astrophys. J. Suppl., 131*, 273-334.

Gammie C. F. (1996) *Astrophys. J., 457*, 355-362.

Gammie C. F. (2001) *Astrophys. J., 553*, 174-183.

Gilliland R. L., Brown T. M., Guhathakurta P., Sarajedini A., Milone E. F. et al. (2000) *Astrophys. J., 545*, L47-L51.

Goldreich P. and Lynden-Bell D. (1965) *Mon. Not. R. Astron. Soc., 130*, 125-158.

Haghighipour N. and Boss A. P. (2003a) *Astrophys. J., 583*, 996-1003.

Haghighipour N. and Boss A. P. (2003b) *Astrophys. J., 598*, 1301-1311.

Haisch K. E., Lada E. A., and Lada C. J. (2001) *Astrophys. J.*,

*553*, L153-L156.
Inaba S., Wetherill G. W., and Ikoma M. (2003) *Icarus, 166*, 46-62.
Johnson B. M. and Gammie C. F. (2003) *Astrophys. J., 597*, 131-141.
Johnson B. M. and Gammie C. F. (2006) *Astrophys. J., 636*, 63-74.
Johnstone D., Hollenbach D., and Bally J. (1998) *Astrophys. J., 499*, 758-776.
Jones H. R. A. (2004) In *The Search for Other Worlds: Fourteenth Astrophysics Conference, AIP Conference Proceedings, 713*, pp. 17-26. AIP Conference Proceedings, New York.
Klahr H. H. (2003) In *Scientific Frontiers in Research on Extrasolar Planets* (D. Deming and S. Seager, eds.), pp. 277-280. ASP Conference Series, San Francisco.
Klahr H. H. and Bodenheimer P. (2003) *Astrophys. J., 582*, 869-892.
Klahr H. H. and Henning T. (1997) *Icarus, 128*, 213-229.
Kley W. (1999) *Mon. Not. R. Astron. Soc., 303*, 696-710.
Koller J., Li H., and Lin D. N. C. (2003) *Astrophys. J., 596*, L91-94.
Kuiper G. P. (1951) In *Proceedings of a Topical Symposium* (J. A. Hynek, ed.), pp. 357-424. McGraw-Hill, New York.
Lada C. J. and Lada E. A. (2003) *Ann. Rev. Astron. Astrophys., 41*, 57-115.
Larson R. B. (1984) *Mon. Not. R. Astron. Soc., 206*, 197-207.
Laughlin G. and Bodenheimer P. (1994) *Astrophys. J., 436*, 335-354.
Laughlin G. and Różyczka M. (1996) *Astrophys. J., 456*, 279-291.
Laughlin G., Korchagin V., and Adams F. C. (1997) *Astrophys. J., 477*, 410-423.
Laughlin G., Korchagin V., and Adams F. C. (1998) *Astrophys. J., 504*, 945-966.
Laughlin G., Bodenheimer P., and Adams F. C. (2004) *Astrophys. J., 612*, L73-L76.
Laws C., Gonzalez G., Walker K. M., Tyagi S., Dodsworth J. et al. (2003) *Astron. J., 125*, 2664-2677.
Lin D. N. C. and Papaloizou J. C. B. (1993) In *Protostars and Planets III* (E. H. Levy and J. I. Lunine, eds.), pp. 749-835. Univ. of Arizona, Tucson.
Lin D. N. C. and Pringle J. E. (1987) *Mon. Not. R. Astron. Soc., 225*, 607-613.
Lin D. N. C., Laughlin G., Bodenheimer P., and Różyczka M. (1998) *Science, 281*, 2025-2027.
Livio M. and Pringle J. E. (2003) *Mon. Not. R. Astron. Soc., 346*, L42-L44.
Lodato G. and Rice W. K. M. (2004) *Mon. Not. R. Astron. Soc., 351*, 630-642.
Lodato G. and Rice W. K. M. (2005) *Mon. Not. R. Astron. Soc., 358*, 1489-1500.
Lubow S. H. and Ogilvie G. I. (1998) *Astrophys. J., 504*, 983-995.
Lubow S. H., Siebert M., and Artymowicz P. (1999) *Astrophys. J., 526*, 1001-1012.
Lufkin G., Quinn T. Wadsley J., Stadel J., and Governato F. (2004) *Mon. Not. R. Astron. Soc., 347*, 421-429.
Mayer L., Quinn T., Wadsley J., and Stadel J. (2002) *Science 298*, 1756-1759.
Mayer L., Quinn T., Wadsley J., and Stadel J. (2004a) *Astrophys. J., 609*, 1045-1064.
Mayer L., Wadsley J., Quinn T., and Stadel J. (2004b) In *Extrasolar Planets: Today and Tomorrow* (J.-P. Beaulieu et al., eds.), pp. 290-297. ASP Conference Series, San Francisco.
Mayer L., Wadsley J., Quinn T., and Stadel J. (2005) *Mon. Not. R. Astron. Soc., 363*, 641-648.
Mejía A. C. (2004) Ph.D. dissertation, Indiana University.
Mejía A. C., Durisen R. H., Pickett M. K., and Cai K. (2005) *Astrophys. J., 619*, 1098-1113.
Mihalas D. (1977) *Stellar Atmospheres*. Univ. of Chicago, Chicago.
Monaghan J. J. (1992) *Ann. Rev. Astron. Astrophys., 30*, 543-574.
Myhill E. A. and Boss A. P. (1993) *Astrophys. J. Suppl., 89*, 345-359.
Nelson A. F. (2000) *Astrophys. J., 537*, L65-L69.
Nelson A. F. (2006) *Mon. Not. R. Astron. Soc.*, submitted.
Nelson A. F. and Benz W. (2003) *Astrophys. J., 589*, 578-604.
Nelson A. F., Benz W., Adams F. C., and Arnett D. (1998) *Astrophys. J., 502*, 342-371.
Nelson A. F., Benz W., and Ruzmaikina T. V. (2000) *Astrophys. J., 529*, 357-390.
Nelson R. P., Papaloizou J. C. B., Masset F., and Kley W. (2000) *Mon. Not. R. Astron. Soc., 318*, 18-36.
Neuhäuser R., Guenther E. W., Wuchterl G., Mugrauer M., Bedalov A., and Hauschildt P. H. (2005) *Astron. Astrophys., 435*, L13-L16.
Osorio M., D'Alessio P., Muzerolle J., Calvet N., and Hartmann L. (2003) *Astrophys. J., 586*, 1148-1161.
Paczyński B. (1978) *Acta Astron., 28*, 91-109.
Papaloizou J. C. B. and Savonije G. (1991) *Mon. Not. R. Astron. Soc., 248*, 353-369.
Paulson D. B., Saar S. H., Cochran W. D., and Henry G. W. (2004) *Astron. J., 127*, 1644-1652.
Pickett B. K. (1995) Ph.D. dissertation, Indiana University.
Pickett B. K., Durisen R. H., and Davis G. A. (1996) *Astrophys. J., 458*, 714-738.
Pickett B. K., Cassen P., Durisen R. H., and Link R. P. (1998) *Astrophys. J., 504*, 468-491.
Pickett B. K., Cassen P., Durisen R. H., and Link R. P. (2000a) *Astrophys. J., 529*, 1034-1053.
Pickett B. K., Durisen R. H., Cassen P., and Mejía A. C. (2000b) *Astrophys. J., 540*, L95-98.
Pickett B. K., Mejía A. C., Durisen R. H., Cassen P. M., Berry D. K., and Link R. P. (2003) *Astrophys. J., 590*, 1060-1080.
Podolak M. (2003) *Icarus, 165*, 428-437.
Pollack J. B., Hubickyj O., Bodenheimer P., Lissauer J. J., Podolak M., and Greenzweig Y. (1996) *Icarus, 124*, 62-85.
Pringle J. E. (1981) *Ann. Rev. Astron. Astrophys., 19*, 137-162.
Rafikov R. R. (2005) *Astrophys. J., 621*, L69-L72.
Rice W. K. M., Armitage P. J., Bate M. R., and Bonnel I. A. (2003a) *Mon. Not. R. Astron. Soc., 338*, 227-232.
Rice W. K. M., Armitage P. J., Bate M. R., and Bonnell I. A. (2003b) *Mon. Not. R. Astron. Soc., 339*, 1025-1030.
Rice W. K. M., Armitage P. J., Bate M. R. and Bonnell I. A. (2003c) *Mon. Not. R. Astron. Soc., 346*, L36-L40.
Rice W. K. M., Lodato G., and Armitage P. J. (2005) *Mon. Not. R. Astron. Soc., 364*, L56-L60.
Rice W. K. M., Lodato G., Pringle J. E., Armitage P. J., and Bonnell I. A. (2004) *Mon. Not. R. Astron. Soc., 355*, 543-552.
Rodríguez L. F., Loinard L., D'Alessio P., Wilner D. J., and Ho P. T. P. (2005) *Astrophys. J., 621*, 133-136.
Ruden S. P. and Pollack J. B. (1991) *Astrophys. J., 375*, 740-760.
Santos N. C., Israelian G., and Mayor M. (2004) *Astron. Astrophys., 415*, 1153-1166.
Sato B., Fischer D. A., Henry G. W., Laughlin G., Butler R. P. et al. (2005) *Astrophys. J., 633*, 465-473.
Saumon D. and Guillot T. (2004) *Astrophys. J., 609*, 1170-1180.

Shu F. H., Tremaine S., Adams F. C., and Ruden S. P. (1990) *Astrophys. J., 358*, 495-514.
Sigurdsson S., Richer H. B., Hansen B. M., Stairs I. H., and Thorsett S. E. (2003) *Science, 301*, 193-196.
Springel V. (2005) *Mon. Not. R. Astron. Soc., 364*, 1105-1134.
Springel V., Yoshida N., and White S. D. M. (2001) *New Astron., 6*, 79-117.
Sozzetti A. (2004) *Mon. Not. R. Astron. Soc., 354*, 1194-1200.
Stone J. M. and Norman M. L. (1992) *Astrophys. J. Suppl., 80*, 753-790.
Tanaka H., Himeno Y., and Ida S. (2005) *Astrophys. J., 625*, 414-426.
Tohline J. E. (1980) *Astrophys. J., 235*, 866-881.
Toomre A. (1964) *Astrophys. J., 139*, 1217-1238.
Tomley L., Cassen P., and Steiman-Cameron T. Y. (1991) *Astrophys. J., 382*, 530-543.
Truelove J. K., Klein R. I., McKee C. F., Holliman J. H. II, Howell L. H., and Greenough J. A. (1997) *Astrophys. J., 489*, L179-L183.
Wadsley J., Stadel J., and Quinn T. (2004) *New Astron., 9*, 137-158.
Weidenschilling S. J. (1977) *Mon. Not. R. Astron. Soc., 180*, 57-70.
Weidenschilling S. J. and Cuzzi J. N. (1993) In *Protostars and Planets III* (E. H. Levy and J. I. Lunine, eds.), pp. 1031-1060. Univ. of Arizona, Tucson.
Yorke H. W. and Bodenheimer P. (1999) *Astrophys. J., 525*, 330-342.
Youdin A. N. and Shu F. H. (2002) *Astrophys. J., 580*, 494-505.